THE JOURNAL OF BIOLOGICAL CHEMISTRY VOL. 287, NO. 51, pp. 42502–42515, December 14, 2012

Artemin Stimulates Radio- and Chemo-resistance by Promoting TWIST1-BCL-2-dependent Cancer Stem Cell-like Behavior in Mammary Carcinoma Cells*[S]

Received for publication, March 21, 2012, and in revised form, October 16, 2012 Published, JBC Papers in Press, October 24, 2012, DOI 10.1074/jbc.M112.365163

Arindam Banerjee[‡1], PengXu Qian[§1], Zheng-Sheng Wu[§¶‖], Xiaoge Ren[‡], Michael Steiner[‡], Nicola M. Bougen[**], Suling Liu[§], Dong-Xu Liu[‡], Tao Zhu[§2], and Peter E. Lobie[‡3]**

*From the [‡]Liggins Institute, University of Auckland, Auckland 1023, New Zealand, [§]Hefei National Laboratory for Physical Sciences at Microscale and School of Life Sciences, University of Science and Technology of China, Hefei, Anhui 230027, China, the [¶]Department of Pathology, Anhui Medical University, Hefei, Anhui, China, the [‖]Department of Pathology, Shanghai Medical College, Fudan University, Shanghai, China, the **Cancer Science Institute of Singapore and Department of Pharmacology, National University of Singapore, Singapore 117599*

Background: Artemin is an oncogenic and metastatic factor in mammary carcinoma.
Results: Artemin promotes radio- and chemo-resistance by enhancing TWIST1-BCL-2-dependent cancer stem cell like behavior in mammary carcinoma cells.
Conclusion: Artemin functions as a cancer stem cell (CSC) factor in mammary carcinoma cells.
Significance: Functional inhibition of ARTN may be useful to inhibit CSC activity in mammary carcinoma.

Artemin (ARTN) has been reported to promote a TWIST1-dependent epithelial to mesenchymal transition of estrogen receptor negative mammary carcinoma (ER-MC) cells associated with metastasis and poor survival outcome. We therefore examined a potential role of ARTN in the promotion of the cancer stem cell (CSC)-like phenotype in mammary carcinoma cells. Acquired resistance of ER-MC cells to either ionizing radiation (IR) or paclitaxel was accompanied by increased ARTN expression. Small interfering RNA (siRNA)-mediated depletion of ARTN in either IR- or paclitaxel-resistant ER-MC cells restored cell sensitivity to IR or paclitaxel. Expression of ARTN was enriched in ER-MC cells grown in mammospheric compared with monolayer culture and was also enriched along with *BMI1*, *TWIST1*, and *DVL1* in mammospheric and ALDH1+ populations. ARTN promoted mammospheric growth and self-renewal of ER-MC cells and increased the ALDH1+ population, whereas siRNA-mediated depletion of ARTN diminished these CSC-like cell behaviors. Furthermore, increased ARTN expression was significantly correlated with ALDH1 expression in a cohort of ER-MC patients. Forced expression of ARTN also dramatically enhanced tumor initiating capacity of ER-MC cells in xenograft models at low inoculum. ARTN promotion of the CSC-like cell phenotype was mediated by TWIST1 regulation of BCL-2 expression. ARTN also enhanced mammosphere formation and the ALDH1+ population in estrogen receptor-positive mammary carcinoma (ER+MC) cells. Increased expression of ARTN and the functional consequences thereof may be one common adaptive mechanism used by mammary carcinoma cells to promote cell survival and renewal in hostile tumor microenvironments.

Despite advances in the diagnosis and treatment of mammary carcinoma, the ER[4] negative subtype of mammary carcinoma (ER-MC) remains associated with worse overall and disease-free survival outcomes compared with other types of mammary carcinoma (1, 2). Furthermore, ER-MC is composed almost entirely of "triple-negative" mammary carcinoma (*i.e.* tumors that are negative for ER, progesterone receptor, and HER-2) that are also associated with poor clinical outcome (2). Thus, further study is warranted to more effectively target this clinically challenging subgroup of mammary carcinoma. In addition to ER-MC, ER-positive mammary carcinoma (ER+MC) that has acquired resistance to anti-estrogens also poses a particular clinical challenge, with an overwhelming poor outcome (3, 4).

Recently, reports have revealed the existence of a subpopulation of tumor-initiating cells known as cancer stem cells (CSCs) (5). These CSCs are proposed to be responsible for

* This work was funded by the Breast Cancer Research Trust (New Zealand), The Dick Roberts Trust (New Zealand), Cancer Science Institute (Singapore), The National Key Scientific Programme of China (2012CB934002 and 2010CB912804), Chinese Academy of Sciences (XDA1040410), National Natural Science Foundation of China (30971492 and 81101597), and the Chinese Academy of Sciences Visiting Professorship for Senior International Scientists (2010T2S03). D.-X. L. and P. E. L. are inventors of PCT/NZ2008/000152 and derivatives thereof. P. E. L. is an inventor of PCT/NZ2010/000207 and derivatives thereof. Z. T. and P. E. L. received consultancies from Saratan Therapeutics Ltd (a biotech company formed around the potential to use Artemin as a target for breast cancer). Salaries of D.-X. L. and A. B. were supported in part by Saratan Therapeutics Ltd.
[S] This article contains supplemental Figs. S1–S4.
[1] Both authors contributed equally.
[2] To whom correspondence should be addressed. Tel.: 86-5513601505; E-mail: zhut@ustc.edu.cn.
[3] To whom correspondence should be addressed: Cancer Science Institute of Singapore, National University of Singapore, Centre for Life Sciences, #03-06C, 28 Medical Dr., Singapore 117456. Tel.: 65-66011046; E-mail: csipel@nus.edu.sg.

[4] The abbreviations used are: ER, estrogen receptor; ER-MC, ER-negative subtype of mammary carcinoma; ARTN, artemin; CSC, cancer stem cell; GFL, GDNF family ligand; IR, ionizing radiation; IRR, ionizing radiation-resistant; PTXR, paclitaxel resistant; qPCR, quantitative real time PCR; Gy, gray; GDNF, glial cell line derived neurotrophic factor.

tumor initiation, growth, epithelial-mesenchymal transition (EMT), and metastasis (6, 7) and also promote a radio- and chemo-resistant cancer phenotype (5, 8), thereby abrogating complete therapeutic elimination of the tumor (9). For example, a recent study on one ER-molecular subtype of mammary carcinoma associated with poor survival, the claudin-low subtype, demonstrated higher expression of genes involved in EMT, such as *SNAI1* and *TWIST1*, and also enhanced stem cell-like features (10, 11). Hence, understanding the basic molecular mechanism of CSC functioning and the identification of CSC-specific markers is essential to develop targeted therapeutics to maximize the clinical response of subgroups of mammary carcinoma with poor outcome to different therapeutic strategies (12).

Artemin (ARTN) is a member of the GDNF family of secreted ligands (4). ARTN has been reported to promote oncogenicity in mammary carcinoma, and tumor expression of ARTN is associated with residual disease after chemotherapy, metastasis, relapse, and death (13). We have also reported that ARTN increases TWIST1 to promote EMT and metastasis in ER-MC and that combined low tumor expression of both ARTN and TWIST1 predicted 100% survival in patients with ER-MC (14). Furthermore, we have observed that ARTN expression predicts poor survival of ER+MC patients treated with tamoxifen and that ARTN promotes resistance to antiestrogens in mammary carcinoma, which is mediated by BCL-2 (4), and also to chemotherapeutic agents in endometrial carcinoma (15). Moreover, depletion of ARTN reverses acquired tamoxifen resistance in mammary carcinoma cells (4). Given that recent reports also suggest that TWIST1 (16) and BCL-2 (17) promote CSC-like behavior in mammary carcinoma, we postulate that ARTN may execute its cellular effects by modulation of a CSC-like cell population. In this report we have demonstrated the functional involvement of ARTN in radio- and chemo-resistance by a TWIST1-BCL-2-dependent increase in the CSC-like cell population in mammary carcinoma cells.

EXPERIMENTAL PROCEDURES

Cell Culture—Cell lines used in this study were obtained from the ATCC (American Type Culture Collection) and were cultured as recommended. Generation of MDA-MB-231 and BT549 cells with forced or depleted expression of ARTN has been previously described (14).

For irradiation-resistant (IRR) cell line generation, each flask was irradiated with cobalt$_{60}$ γ-radiation at an average dose of 4 Gy, and the cells were returned to the incubator. After 48 h cells were trypsinized and subcultured to a new flask. When cell confluence reached ~50%, the cells were again irradiated. This cycle was repeated until we observed significant IRR (4 Gy) after assessing cell viability after IR treatment. The paclitaxel resistant cell lines were grown under selective pressure (IC_{50} of each cell line) for 3 days and subsequently for 3 days without paclitaxel. This cycle was repeated until we observed significant paclitaxel resistance of paclitaxel-treated BT549 cells by assessing cell viability after paclitaxel treatment.

Reagents—Paclitaxel was purchased from Sigma. Epidermal growth factor (EGF), basic FGF, bovine insulin, and B27 were from Invitrogen. The Aldefluor assay kit was purchased from Stem Cell Technologies (Melbourne, Australia). Low melting agarose and *N*-lauroylsarcosine sodium salt were purchased from Sigma.

Quantitative PCR—qPCR was performed as described earlier (14). BMI1 primers used for qPCR were forward (5′-TGGACTGACAAATGCTGGAG-3′) and reverse (5′-GGCAAACAAGAAGAGGTGGA-3′). DVL1 primers used for qPCR were forward (5′-CCTCCTTCAGCAGCATAACC-3′) and reverse (5′-GCTGATGCCCAGAAAGTGAT-3′). ALDH1 primers used for qPCR were forward (5′-TCGTCTGCTGCTGGCGACAATG-3′) and reverse (5′-CCCAACCTGCACAGTAGCGCAA-3′). CD44 primers used for qPCR were forward (5′-ACACCATGGACAAGTTTTGGTG-3′) and reverse (5′-CTGCAGGTCTCAAATCCGATG-3′). Other primers, which include ARTN (4), TWIST1 (14), CD24 (15), CD133 (18), and BCL-2 (13), were as previously published.

Luciferase Reporter Assay—Luciferase reporter assay was performed as described previously (19) using TWIST1 (20) and BCL-2 (19) promoter constructs.

Immunoblotting—Western blot analysis was performed as described earlier (21). Western blot analysis was performed using the following antibodies: goat ARTN polyclonal antibody (R&D Systems, Minneapolis, MN), mouse β-actin monoclonal antibody (Sigma), rabbit TWIST1 polyclonal antibody (Santa Cruz), and mouse BCL-2 monoclonal antibody (Invitrogen).

Comet Assay—A comet assay to evaluate DNA damage by single cells gel electrophoresis assay was performed as described earlier (22). The comet tails were analyzed by CometScore™ software.

Clonogenic Assay—Radiation sensitivities of the cell lines were determined by measuring colony formation after cells were exposed to ionizing radiation as previously described (23). Exponentially growing MDA-MB-231 and BT549-ARTN cells were irradiated with 4 Gy-ionizing radiation. 24 h post irradiation cells were trypsinized, plated in 6-well plates in triplicate at 400 cells per well, and cultured in full serum media for 14 days. After 14 days, the cells were washed with 1 ml of PBS and then fixed in 500 μl of methanol for 20 min. The colonies were stained with 0.1% crystal violet in 20% ethanol (in PBS) for 30 min at room temperature. Colonies of >50 cells were counted. Surviving fractions were normalized by the plating efficiency of unirradiated controls (23).

Aldefluor Assay—An Aldefluor assay was performed as per the manufacturer's instruction. In brief, surviving cell populations were harvested in 0.25% trypsin and collected by gentle centrifugation. Cell pellets were then washed twice in PBS. Cells were then resuspended in Aldefluor assay buffer containing ALDH substrate BODIPY® aminoacetaldehyde (BAAA, 1 μmol/liter/1 $\times$ 10^6 cells) and incubated for 40 min at 37 °C. As negative control, for each sample of cells, an aliquot was treated with 50 mmol/liter diethylaminobenzaldehyde, a specific ALDH inhibitor. Flow cytometry was performed using FACSAria™ II instrument (BD Biosciences) (Faculty of Medical and Health Sciences, The University of Auckland).

CD24/44 Cell Surface Markers Staining—After 30 min of incubation with Aldefluor reagent, 5 μl of CD24-PE and 2.5 μl of CD44-PerCP-Cy 5.5 (both from BD Pharmingen™) were directly added to the sample mixture and incubated for 20 min

at room temperature in the dark. Respective isotype control antibodies were also added in control tubes. After centrifugation and washing, the respective cell pellets were resuspended in 400 μl of Aldefluor buffer for further analysis.

Mammosphere Assay—Monolayer cells were harvested in trypsin-EDTA and carefully resuspended in Dulbecco's modified Eagle's medium F12 (Invitrogen) supplemented with 20 ng/ml recombinant human EGF, 20 ng/ml recombinant human basic FGF, B27 supplement, 0.4% FBS, penicillin-streptomycin, L-glutamine (all from Invitrogen), and 5 μg/ml bovine insulin (Sigma). The suspensions were passed through a 35-μm nylon filter and assessed under a light microscope to confirm cell disaggregation. Single cells were plated in ultra low attachment plates (Corning, MA) at a density of 2000 cells/100 μl in a 96-wellplate format, subsequent passages were grown as 1000 cells/100 μl, and viability was measured by alamarBlue (Invitrogen) as described previously (24).

Cell Function Assays—Soft agar colony formation assay, three-dimensional cell growth, cell migration, and invasion assays were performed as previously described (13). For monolayer cell proliferation, 3000 cells were seeded into 100 μl of media (2% FBS), and after 72 h viability was quantified as described previously (14).

Tumor Xenograft in Nude Mice—All animal work was done in accordance with a protocol approved by the institutional animal care and ethics committee of The University of Science and Technology of China. Tumor growth assays were performed as described earlier (14).

Histopathological Analysis—Tissue samples were collected with informed consent from 94 female ER-MC patients from the First Affiliated Hospital of Anhui Medical University (Hefei, China) presenting between 2001 and 2002 (14). Institutional ethics committee approval for the project was obtained before commencement of the study and was in compliance with the Helsinki Declaration. Immunohistochemical analysis of paraffin-embedded specimens was performed as described previously (14).

RNA Analysis—RNA was extracted by TRIzol® Plus RNA Purification system from 24 ER-MC patients with invasive mammary ductal carcinoma who underwent surgery at the First Affiliated Hospital of Anhui Medical University (Hefei, China) between 2001 and 2002. All patients were Han Chinese female. The histopathological diagnosis of the specimens was consistent with breast neoplasm in accordance with World Health Organization guidelines. The protocol for use of tissue samples was approved by the institutional review board, and written informed consent was obtained from each patient. SYBR Premix Ex Taq kit (Takara) was used to determine the expression levels of ARTN, BCL-2, and ALDH1. The relative amount of gene transcripts was normalized to GAPDH. The Pearson correlation coefficient was used to analyze the correlation between the expression levels of ARTN, BCL-2, and ALDH1.

Statistics—All numerical data are expressed as the mean ± S.E., and statistical significance was assessed by Student's *t* test ($p < 0.05$ was considered as significant) using Microsoft Excel XP unless otherwise indicated (χ^2 test).

RESULTS

ARTN Modulates Sensitivity to Ionizing Radiation and Paclitaxel in ER-MC—One feature of the CSC-like phenotype is reduced sensitivity to sublethal doses of ionizing irradiation (IR) (8). To determine the effect of ARTN expression on IR sensitivity in ER-MC, we generated stable MDA-MB-231 and BT549 cell clones with either forced expression or siRNA-mediated depletion of ARTN as previously described (14). Differences in monolayer proliferation on exposure to a sublethal dose of IR were evident with forced expression or depletion of ARTN in MDA-MB-231 and BT549 cells compared with their respective control cells (Fig. 1*A*). The replicative competence of MDA-MB-231-ARTN and BT549-ARTN cells after IR exposure was determined in standard radiation clonogenic assays (23). Cells with forced expression of ARTN readily formed a higher number of colonies compared with their respective control VEC cells. Depletion of ARTN in MDA-MB-231 and BT549 cells resulted in a lower number of colonies compared with their respective control siCONT cells (Fig. 1*B*). As IR-induced cell death is generally attributed to primary DNA damage (8), Comet assays were performed to detect DNA damage. Comet tails, representing a significant fraction of unrepaired genomic DNA damage (25), were significantly higher in MDA-MB-231-VEC and BT549-VEC cells compared with the MDA-MB-231-ARTN and BT549-ARTN cells at 15 min and 1 h post-IR, indicating that ARTN reduced DNA damage consequent to exposure to IR (Fig. 1*C*). Depletion of ARTN in MDA-MB-231 and BT549 cells produced significantly longer comet tails compared with the respective siCONT cells at 15 min and 1 h post IR (Fig. 1*D*).

To determine whether ARTN possesses a functional role in acquired resistance to IR, we developed an IRR MDA-MB-231 cell line by fractionated irradiation of 4Gy for 12 cycles as described earlier (26). MDA-MB-231-IRR cells differed from the wild type (WT) cells in their sensitivity to IR (4 Gy) by 1.8-fold (Fig. 1*F*). Protein levels of ARTN were higher in IRR cells compared with wild type cells both with and without IR treatment (Fig. 1*E*, *upper panel*). To determine the functional consequences of the increased ARTN expression in IRR cells, we employed siRNA to reduce ARTN expression in both MDA-MB-231-WT and -IRR cells. Depletion of ARTN by siRNA significantly decreased ARTN expression in both IRR and WT cells (Fig. 1*E*, *lower panel*). Depletion of ARTN reduced the viability of MDA-MB-231-WT cells upon exposure to a sublethal dose of IR. Depletion of ARTN also abrogated the enhanced resistance to IRR observed in IRR-resistant cells, reducing cell viability upon IR treatment to that observed in WT cells (Fig. 1*F*). Forced expression of ARTN has previously been reported to increase MDA-MB-231 cell growth in three-dimensional Matrigel (14). MDA-MB-231-IRR cells exhibited increased cell growth in three-dimensional Matrigel in comparison to WT cells (Fig. 1*G*). Depletion of ARTN reduced the basal capacity for growth of MDA-MB-231-WT cells and also prevented the enhanced growth of IRR cells in three-dimensional Matrigel. Depletion of ARTN in MDA-MB-231-WT cells resulted in further reduction of cell growth in three-dimensional Matrigel in response to IR. Furthermore, depletion

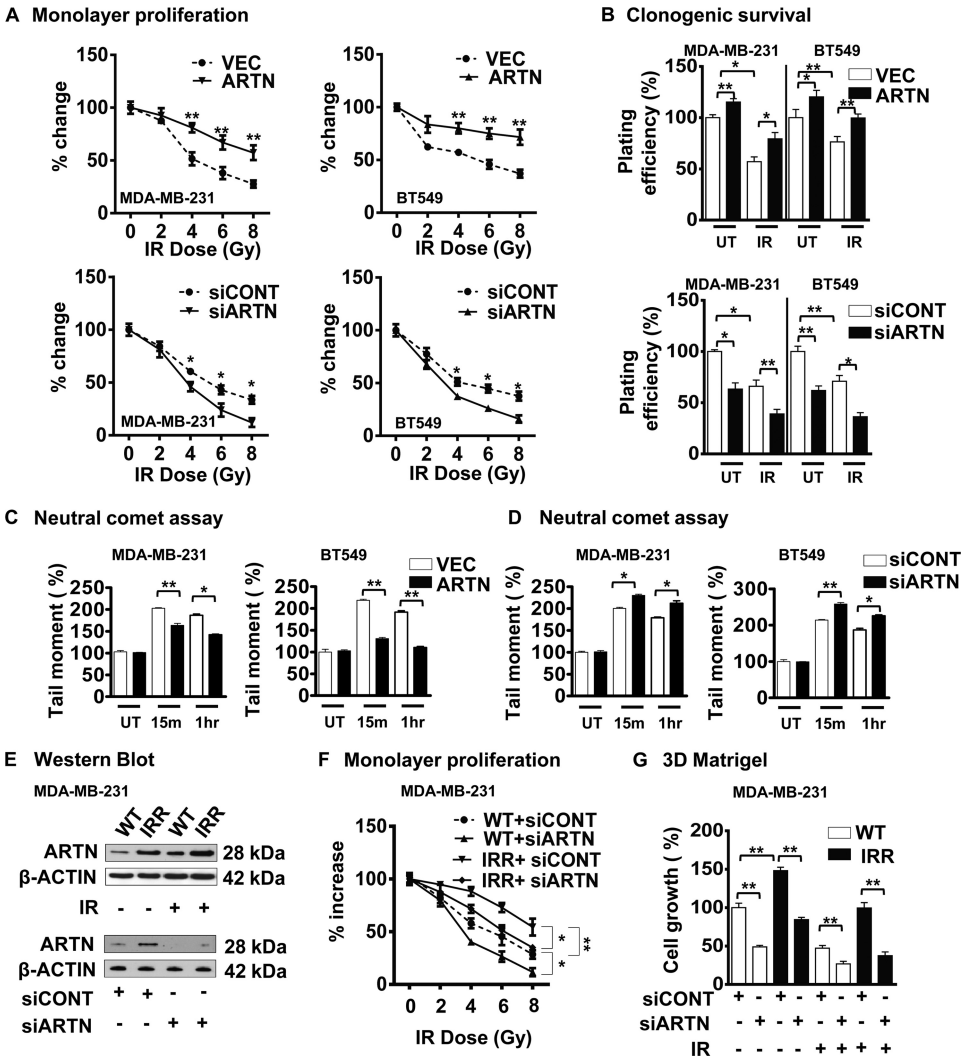

FIGURE 1. **ARTN possesses a functional role in acquired resistance of ER-MC cells to IR.** *A*, shown is monolayer proliferation assay. MDA-MB-231 and BT549 cells with forced or depleted expression of ARTN were either untreated or exposed to various sub lethal doses of IR. After 24 h cells were seeded in 2% serum-containing media, and cell viability was measured by alamarBlue after 72 h. *B*, clonogenic survival is shown. MDA-MB-231 and BT549 cells with forced or depleted expression of ARTN were either untreated or exposed to a 4-Gy dose of IR, and 24 h later, 600 cells/well were seeded in 10% serum-containing media in 6-well plates. After 2 weeks colonies with greater than 50 cells were counted by crystal violet stain, and plating efficiencies were calculated (number of colonies formed/number of cells seeded × 100). *C*, shown is a neutral comet assay. MDA-MB-231 and BT549 cells with forced expression of ARTN were treated with a 4-Gy dose of IR, and DNA double-stranded breaks were measured using the neutral comet assay. The tail moment correlates with the level of DSBs present in untreated (*UT*) cells; cells were at 15-min post IR (*15m*) and at 1 h post IR (*1h*). *D*, a neutral comet assay is shown. MDA-MB-231 and BT549 cells with depleted expression of ARTN were treated with a 4-Gy dose of IR, and DNA double-stranded breaks were measured using the neutral comet assay. The tail moment correlates with the level of DSBs present in untreated (*UT*) cells; cells were at 15 min post-IR and at 1 h post-IR. *E*, Western blot analysis for ARTN protein expression in WT and IRR MDA-MB-231 cells ± IR. β-ACTIN was used as a loading control (*upper panel*). Western blot analysis for ARTN in WT and IRR MDA-MB-231 cells ± siRNA to ARTN demonstrate efficiency of siRNA-mediated depletion of ARTN protein (*lower panel*). *F*, shown is monolayer proliferation assay is shown. WT and IRR MDA-MB-231 cells were cultured in 2% serum containing media and treated with different doses of IR ± siRNA to ARTN. After 72 h cell viability was measured by alamarBlue. *G*, shown is cell growth in three-dimensional Matrigel of MDA-MB-231- WT and -IRR cells ± IR ± siRNA to ARTN. *, $p < 0.05$; **, $p < 0.01$.

of ARTN completely abrogated the three-dimensional Matrigel growth advantage of IRR cells in response to IR when compared with WT cells (Fig. 1*G*).

CSC-like cells also exhibit increased resistance to chemotherapeutic agents such as paclitaxel (5). Concordantly, we observed that ARTN modulated paclitaxel sensitivity in ER-MC cells. Forced expression of ARTN abrogated the reduction in both MDA-MB-231 and BT549 cell viability in response to increasing concentration of paclitaxel (IC_{50}; MDA-MB-231-VEC, 5.4 ± 0.29 nM; MDA-MB-231-ARTN, 10.63 ± 0.13 nM; BT549-VEC, 24.61 ± 0.37 nM; BT549-ARTN, 36.99 ± 0.11 nM) (Fig. 2*A*). siRNA-mediated depletion of ARTN in MDA-MB-231 and BT549 cells enhanced sensitivity to paclitaxel (IC_{50}; MDA-MB-231-siCONT, 5.1 ± 0.15 nM; MDA-MB-231-siARTN, 3.1 ± 0.11 nM; BT549-siCONT, 24.74 ± 0.20 nM; BT549-siARTN, 18.58 ± 0.36 nM) (Fig. 2*A*). We also examined the effect of paclitaxel (IC_{50}, MDA-MB-231–5 nM and BT549–24 nM) on three-dimensional Matrigel growth of MDA-MB-231 and BT549 cells with forced or depleted expression of ARTN. Forced expression of ARTN enhanced three-dimensional Matrigel growth of both cell lines and partially prevented the inhibition of three-dimensional cell growth consequent to paclitaxel treatment (Fig. 2*B*). Depletion of ARTN reduced growth of both cell lines in three-dimensional Matrigel

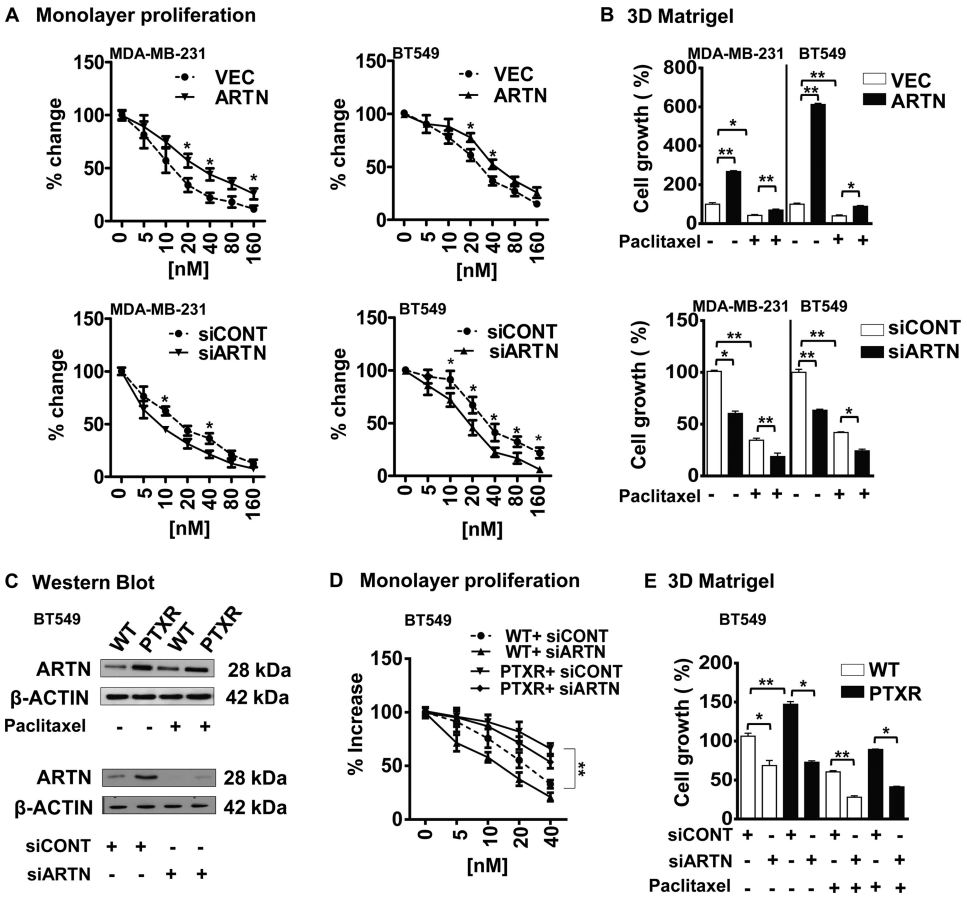

FIGURE 2. **ARTN possesses a functional role in acquired resistance to paclitaxel in ER-MC cells.** *A*, shown is a monolayer proliferation assay. MDA-MB-231 and BT549 cells with forced or depleted expression of ARTN were seeded in 2% serum containing media with different concentrations of paclitaxel. After 72 h, cell viability was measured by alamarBlue. *B*, shown is cell growth in three-dimensional Matrigel of MDA-MB-231 and BT549 cells with forced or depleted expression of ARTN ± paclitaxel. After 10 days, cell growth was measured by alamarBlue. DMSO-treated control cells are presented as 100%. *C*, Western blot analysis for ARTN protein expression in WT and paclitaxel-resistant (PTXR) BT549 cells ± paclitaxel is shown. β-Actin was used as a loading control (*upper panel*). Western blot analysis for ARTN in WT and PTXR cells ± siRNA to ARTN demonstrates the efficacy of siRNA-mediated depletion of ARTN (*lower panel*). *D*, shown is a monolayer proliferation assay. BT549-WT and -PTXR cells were seeded in 2% serum-containing media with different concentrations of paclitaxel ± siARTN. After 3 days cell viability was measured by alamarBlue. *E*, shown is cell growth in three-dimensional Matrigel of BT549-WT and -PTXR cells ± paclitaxel ± siRNA to ARTN. DMSO-treated control cells are presented as 100%. All others parameters are presented compared with respective control cells. *, $p < 0.05$; **, $p < 0.01$.

and enhanced the growth inhibitory effects of paclitaxel treatment (Fig. 2*B*).

To determine a potential role for ARTN in acquired resistance to paclitaxel, we developed a paclitaxel-resistant (PTXR) BT549 cell line (27). Western blot analysis demonstrated higher expression of ARTN protein in PTXR cells compared with respective wild type cells both with or without paclitaxel treatment (Fig. 2*C*, *upper panel*). BT549-PTXR cells exhibited enhanced growth in both monolayer and three-dimensional Matrigel (24 nM paclitaxel) in comparison to WT cells (Fig. 2, *D* and *E*). To determine a functional contribution of increased ARTN expression in PTXR cells, we employed siRNA to reduce ARTN expression in both BT549-WT and -PTXR cells. Depletion of ARTN by siRNA significantly decreased ARTN protein expression in both PTXR and WT cells (Fig. 2*C*, *lower panel*). Depletion of ARTN reduced the monolayer viability of WT cells in response to paclitaxel (Fig. 2*D*). Depletion of ARTN also abrogated the enhanced resistance to paclitaxel observed in PTXR cells, reducing cell viability upon paclitaxel treatment to that observed in WT cells (Fig. 2*D*). Depletion of ARTN reduced the basal capacity for growth of BT549-WT cells and also prevented the enhanced growth of PTXR cells in three-dimensional Matrigel. Depletion of ARTN in BT549-WT cells resulted in further reduction of growth in three-dimensional Matrigel in response to paclitaxel. Furthermore, depletion of ARTN abrogated the three-dimensional Matrigel growth advantage of PTXR cells in the presence to paclitaxel when compared with WT cells (Fig. 2*E*).

Increased Expression of ARTN in a CSC-rich Population from ER-MC—To determine a potential role of ARTN in the ER-MC CSC-like population, MDA-MB-231 and BT549 cells were first grown in mammosphere culture in ultra low attachment plates. Mammospheres are enriched in populations of mammary stem/progenitor cells capable of self-renewal and multi-lineage differentiation (28). Whereas the majority of cells underwent anoikis as expected, some cells displayed the ability to grow as spherical organoids (mammospheres). Mammospheres were isolated, and the expression of ARTN in MDA-MB-231 and BT549 mammospheres was compared with the respective cells grown on monolayer in mammospheric media. The expression of ARTN protein in the mammospheric population of both cell lines was

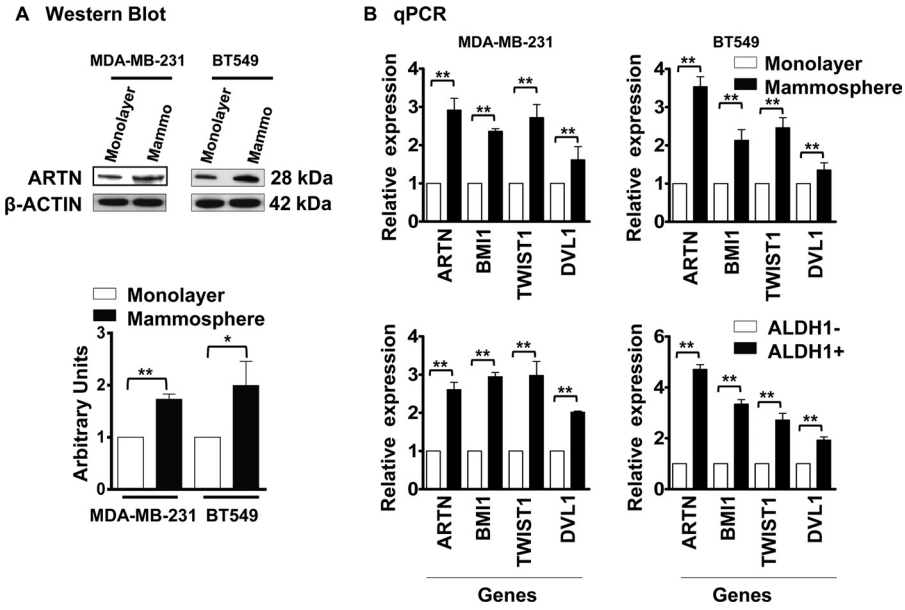

FIGURE 3. **ARTN possesses a functional role in promoting the CSC-like population in ER-MC cells.** *A*, shown is a Western blot analysis for ARTN protein expression in MDA-MB-231 and BT549 cells grown under monolayer and mammospheric conditions respectively. Mammospheric media was used in both conditions, and mammospheres were grown in ultra-low attachment plate. β-Actin was used as a loading control. Protein level was determined by densitometry software (Bio-Rad) and represented as arbitrary units. *B*, shown is increased expression of ARTN in CSC-rich ER-MC cells. Mammosphere and Aldefluor assays were performed to isolate the CSC-rich mammospheric and ALDH1+ population in MDA-MB-231 and BT549 wild type cells, respectively. CSC markers, *BMI1*, *TWIST1*, and *DVL1* and *ARTN* mRNA levels were determined by qPCR and expressed as the relative expression compared with the monolayer (mammosphere/monolayer) or the ALDH1− (ALDH1+/ALDH1−) cell population. *, $p < 0.05$; **, $p < 0.01$.

increased compared with the respective cells grown under adherent monolayer conditions (Fig. 3*A*).

To verify the CSC-like phenotype of mammospheric cells, we examined the mRNA expression of stem cell markers, *BMI1*, *TWIST1*, and *DVL1* (16, 29, 30) and also *ARTN*, in the mammospheres compared with cells grown on monolayer. qPCR analysis of gene expression demonstrated significantly increased mRNA expression of *BMI1*, *TWIST*, *DVL1*, and *ARTN* in mammospheric compared with monolayer grown MDA-MB-231 and BT549 WT cells, respectively (Fig. 3*B*, *upper panel*).

Previous studies have identified the role of ALDH1 as a marker of normal and malignant mammary stem cells (31). We, therefore, similarly utilized the Aldefluor assay to isolate the ALDH1+ and ALDH1− cell populations based on ALDH1 enzymatic activity in MDA-MB-231 and BT549 wild type cells. We examined the mRNA expression of the same stem cell markers and *ARTN* in the ALDH1− and ALDH1+ cell population. qPCR analysis of gene expression demonstrated significantly increased mRNA expression of *BMI1*, *TWIST1*, *DVL1*, and *ARTN* in ALDH1+ cells compared with ALDH1− cells in both MDA-MB-231 and BT549 WT cells, respectively (Fig. 3*B*, *lower panel*).

ARTN Modulates the CSC-like Population in ER-MC Cells—To determine the effect of ARTN on the CSC-like behavior of ER-MC cells, MDA-MB-231 and BT549 cells with forced expression of ARTN were cultured under ultra-low attachment conditions. MDA-MB-231 and BT549 cells with forced expression of ARTN exhibited significantly increased growth (number) of mammospheres compared with the respective VEC cells. Concordantly, we observed decreased mammospheric growth (number) of MDA-MB-231 and BT549 cells with siRNA-mediated depletion of ARTN compared with the siCONT cells, respectively (Fig. 4*A*). To confirm that the increased mammospheric growth represented the progeny of individual cells rather than the aggregation of quiescent cells, we performed self-renewal assays (32). The growth of mammospheres generated upon serial passage provides an indirect measure of mammary stem cell self-renewal (33). We, therefore, examined the ability of primary mammospheres from both MDA-MB-231 and BT549 cells with forced expression of ARTN to form secondary and tertiary mammospheres. The secondary and tertiary mammospheres generated from cells with forced expression of ARTN was significantly increased as compared with those generated from the respective VEC cells (Fig. 4*B*).

To determine if ARTN modulated the ALDH1+ cell population, we measured the ALDH1+ cell number in MDA-MB-231 and BT549 cells with forced or depleted expression of ARTN. Forced expression of ARTN significantly increased the percentage of ALDH1+ cells, whereas siRNA-mediated depletion of ARTN decreased the percentage of ALDH1+ cells (Fig. 4*C*). A previous report demonstrated that ALDH (+)/CD44(+)/CD24(−) and ALDH(+)/CD44(+)/CD133(+) cells are important markers of a CSC population in mammary carcinoma (34). We, therefore, determined if ARTN stimulated alterations in expression of *CD24*, *CD44*, and *CD133* in the ALDH1+ cell population. We utilized the Aldefluor assay to isolate the ALDH1+ cell populations based on ALDH1 enzymatic activity in BT549 cells with forced expression of ARTN and the respective VEC control cells. qPCR analysis of gene expression demonstrated increased mRNA expression of *CD44* and decreased mRNA expression of *CD24* in BT549-ARTN-ALDH1+ cells compared with BT549-VEC-ALDH1+ cells,

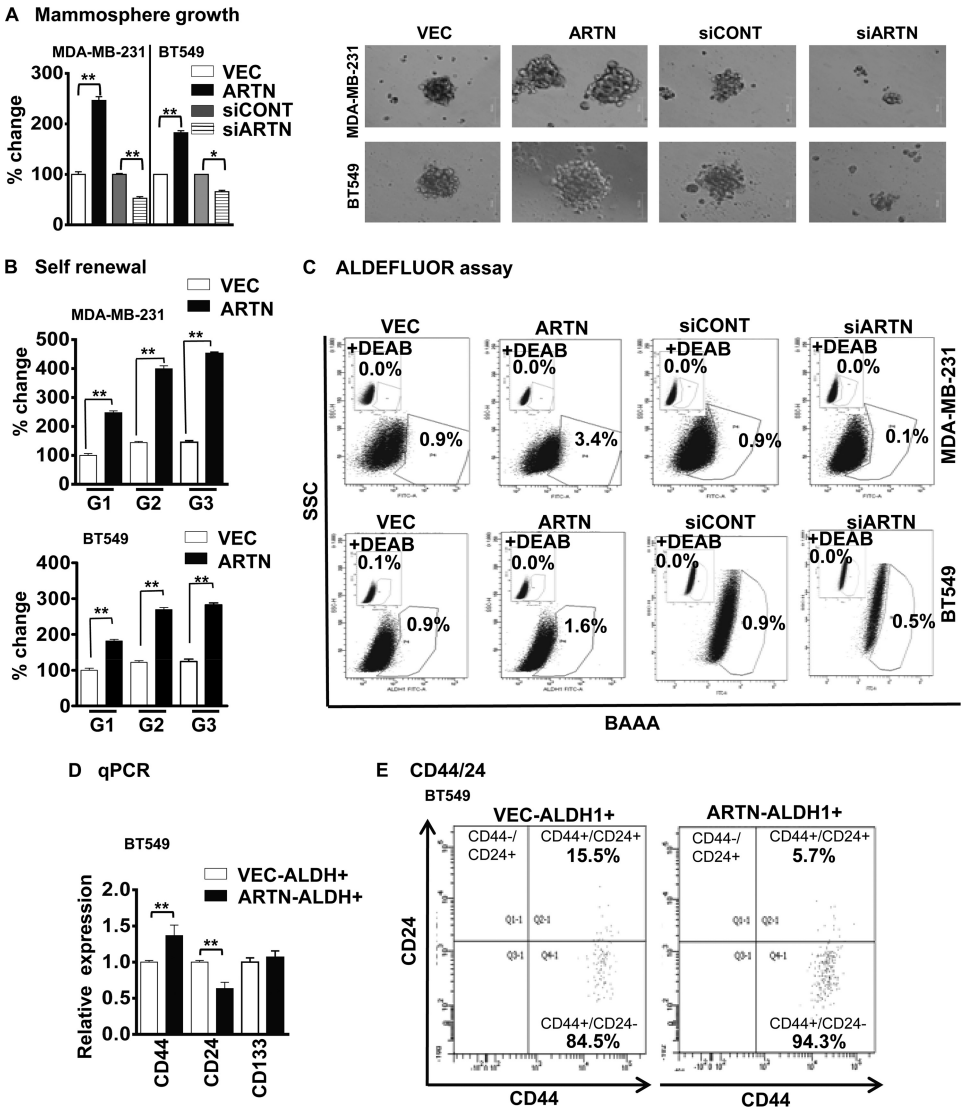

FIGURE 4. **ARTN enhances the CSC-like population in ER-MC cells.** *A*, MDA-MB-231 and BT549 cells with forced or depleted expression of ARTN were seeded in ultra low attachment plates in mammospheric growth media. After 10 days, growth was measured by alamarBlue. Representative images of mammospheres were generated by either forced expression or depleted expression of ARTN cells of MDA-MB-231 and BT549. *Bar*, 50 μm. *B*, ARTN enhanced the self-renewal potential of ER-MC cells. MDA-MB-231 and BT549 cells with forced expression of ARTN were grown under mammospheric conditions and were sequentially cultured from first generation (G1) till third generation (G3), and growth was compared with the respective VEC cells generation. *C*, ARTN modulates ALDH1+ cell population in MDA-MB-231 and BT549 cells with forced or depleted expression of ARTN. Cells were incubated with Aldefluor substrate (BAAA, BODIPY®-aminoacetaldehyde) to define the Aldefluor positive, and a specific inhibitor of ALDH1, diethylaminobenzaldehyde (*DEAB*), was used to establish the base-line fluorescence. Flow cytometry plots indicate side scatter (*SSC*) *versus* fluorescence intensity. *D*, increased expression of mammary CSC markers in the ALDH1+ ER-MC cell population is shown. Aldefluor assays were performed to isolate the ALDH1+ cells in BT549 cells with forced expression of ARTN and the respective control VEC cells. CSC markers, *CD44*, *CD24*, and *CD133* mRNA levels were determined by qPCR and are expressed as the relative expression compared with the VEC-ALDH1+ cell population. *E*, shown is increased expression of mammary CSC markers in CSC-rich ALDH1+ ER-MC cells. BT549 cells with forced expression of ARTN and respective control VEC cells were labeled with the Aldefluor assay kit and fluorescent antibodies (CD24-PE and CD44-PerCP). The Aldefluor assay was performed to isolate the ALDH1+ cells in BT549 cells with forced expression of ARTN and respective control VEC cells, and the ALDH1+ cells were further sorted on the basis of CD44+/CD24− cell surface marker expression. *, $p < 0.05$; **, $p < 0.01$.

respectively (Fig. 4*D*). Next, we also determined if ARTN stimulated alterations of CD44 and CD24 cell surface expression markers in the ALDH1+ cell population. We utilized the Aldefluor assay to isolate the ALDH1+ cell populations based on ALDH1 enzymatic activity in BT549 cells with forced expression of ARTN and the respective VEC control cells as the primary sort criteria. The resulting ALDH1+ cells sorted from both BT549-VEC and -ARTN clones were further gated for CD44 and CD24 cell surface markers, and as secondary sort criteria we designated another subset of cells with ALDH1+/CD44+/CD24- expression (34). We observed a significantly increased CD44+/CD24− cell population in the ALDH1+ fraction of BT549 cells with forced expression of ARTN as compared with BT549 VEC cells (Fig. 4*E*).

ARTN Modulates the CSC-like Population in ER+MC Cell—*ARTN* is an estrogen-regulated gene and is also expressed in ER+MC (4). We, therefore, determined if ARTN modulates the CSC-like population in ER+ MCF-7 cells. MCF-7 cells with forced expression of ARTN (13) exhibited significantly increased growth of mammospheres compared with the MCF-7-VEC cells. We also observed that MCF-7 cells with forced expression of ARTN exhibited a significantly increased per-

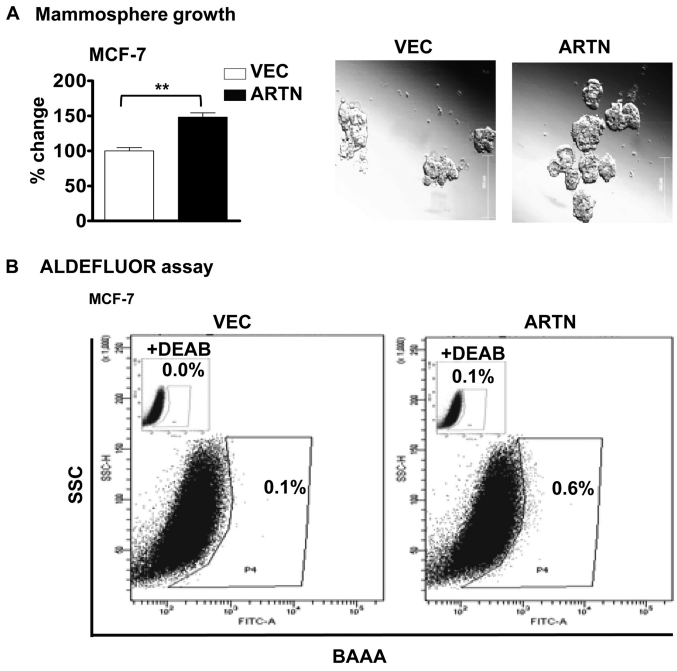

FIGURE 5. **ARTN enhances the CSC-like population in ER+MC cells.** *A*, MCF-7 cells with forced expression of ARTN were seeded in ultra low attachment plates in mammospheric media. After 10 days, growth was measured by alamarBlue. *B*, ARTN increases the ALDH1+ cell population in MCF-7 cells. Shown is a representative bar graph analysis using the FACS analysis of the Aldefluor assay with MCF-7-VEC and MCF-7-ARTN cells. Cells were incubated with Aldefluor substrate (BAAA, BODIPY®-aminoacetaldehyde) to define the Aldefluor-positive, and a specific inhibitor of ALDH1, diethylaminobenzaldehyde (*DEAB*), was used to establish the base-line fluorescence. Flow cytometry plots indicate side scatter (*SSC*) *versus* fluorescence intensity. **, $p < 0.01$.

centage of ALDH1+ cells as compared with MCF-7-VEC cells (Fig. 5, *A* and *B*).

ARTN Enhances Tumor-initiating Capability in ER-MC Cells in Vivo—Another characteristic feature of the CSC-like cell population is enhanced tumor initiating capacity, responsible for metastasis and disease recurrence (35). To determine the effect of forced expression of ARTN on the tumor-initiating capacity of ER-MC cells *in vitro*, we seeded both MDA-MB-231-ARTN and BT549-ARTN cells along with their respective control VEC cells in three-dimensional Matrigel. Cells were seeded at serial dilution (1000 to 125 cells/well). At the lowest cell dilution (125 cells/well), MDA-MB-231 and BT549 cells with forced expression of ARTN still produced 2- and 1.6-fold more cell growth than the VEC cells, respectively (supplemental Fig. S1). We next injected MDA-MB-231-ARTN cells at exponential dilution from 10^5 to 10^2 cells into the mammary fat pad of immunodeficient nude mice and examined their ability to form palpable and measurable tumors as compared with the VEC cells. After 9 weeks, in mice injected with 10^2 cells, palpable tumors were readily detectable in 5/6 mice injected with MDA-MB-231-ARTN cells, whereas only 2/6 mice injected with MDA-MB-231-VEC cells generated palpable tumors. After 9 weeks, in mice injected with 10^3 cells, tumors formed by MDA-MB-231-ARTN cells (5/6) (tumor volume 149.6 ± 61.5 mm^3) were 1.7-fold larger than those formed by the VEC cells (4/6) (tumor volume 88.2 ± 34.2 mm^3). Similarly, after 7.5 weeks in the mice injected with 10^4 or 10^5 cells, 6/6 mice injected with MDA-MB-231-ARTN cells formed tumors that were larger (tumor volume 167.3 ± 91.5 and 274.0 ± 61.0 mm^3, respectively) compared with tumors formed by VEC cells (5/6) (tumor volume 105.9 ± 45.2 and 182.5 ± 76.6 mm^3, respectively) (Table 1).

TABLE 1
Tumor initiating capacity of MDA-MB-231 cells with forced expression of ARTN- and VEC-transfected control cells in immunodeficient mice
Results indicate number of animals in which tumors formed from six animals in each group.

	Number of cells injected			
	10^2	10^3	10^4	10^5
VEC	2/6	4/6	5/6	5/6
ARTN	5/6*	5/6	6/6	6/6

*$p < 0.05$.

BCL-2 Is Necessary for TWIST1-mediated ARTN-stimulated CSC-like Population—BCL-2 has been shown to regulate the CSC-like population in mammary carcinoma cells (17). A previous report also demonstrated that ARTN utilizes BCL-2 to mediate tamoxifen resistance in ER+MC cells (4). We, therefore, determined BCL-2 protein levels in MDA-MB-231 and BT549 cells with forced expression and depletion of ARTN compared with the control VEC cell. Forced expression of ARTN in MDA-MB-231 and BT549 cells significantly increased BCL-2 expression compared with VEC cells (Fig. 6*A*) and as previously reported for ER+MC cells (4). Depletion of ARTN significantly decreased BCL-2 expression in both MDA-MB-231 and BT549 cells compared with their respective siCONT cells (Fig. 6*A*). We previously reported that TWIST1 mediates ARTN stimulated invasion of ER-MC cells (14). ARTN increased TWIST1 expression in BT549 cells by transcriptional regulation via the TWIST1 promoter (supplemental Fig. S2*A*). The transcriptional mechanisms by which TWIST1 regulates BCL-2 expression has previously been determined (36, 37). TWIST1 has been reported to confer chemoresistance by increasing the BCL-2/BAX ratio (36). ARTN increased BCL-2 expression in BT549 cells by transcriptional regulation of the BCL-2 promoter, and siRNA to TWIST1 abrogated ARTN stimulation of the BCL-2 promoter (supplemental Fig. S2*B*). Depletion of TWIST1 by use of siRNA (14) decreased the basal level of BCL-2 expression in MDA-MB-231 cells. siRNA to TWIST1 also significantly decreased the ARTN-stimulated BCL-2 expression in MDA-MB-231-ARTN cells (Fig. 6*B*).

Next we determined TWIST1 and BCL-2 levels in the mammospheric population of MDA-MB-231-ARTN and BT549-ARTN cells compared with the respective VEC mammospheric cell population. Forced expression of ARTN in MDA-MB-231 cells significantly increased both TWIST1 and BCL-2 levels under mammospheric growth conditions compared with the respective VEC cells (Fig. 6*C*).

BCL-2 and TWIST1 has been implicated to possess a role in modulating the CSC-like population in mammary carcinoma cells (16, 17). First, to determine if BCL-2 mediates ARTN enhancement of the CSC-like population, we employed the BCL-2 inhibitor, YC137 (5 μM), to inhibit BCL-2 activity in MDA-MB-231 and BT549 cells with forced expression of ARTN and their respective control VEC cells. Inhibition of BCL-2 abrogated the stimulatory effects of ARTN on mammosphere formation in both MDA-MB-231-ARTN and BT549-

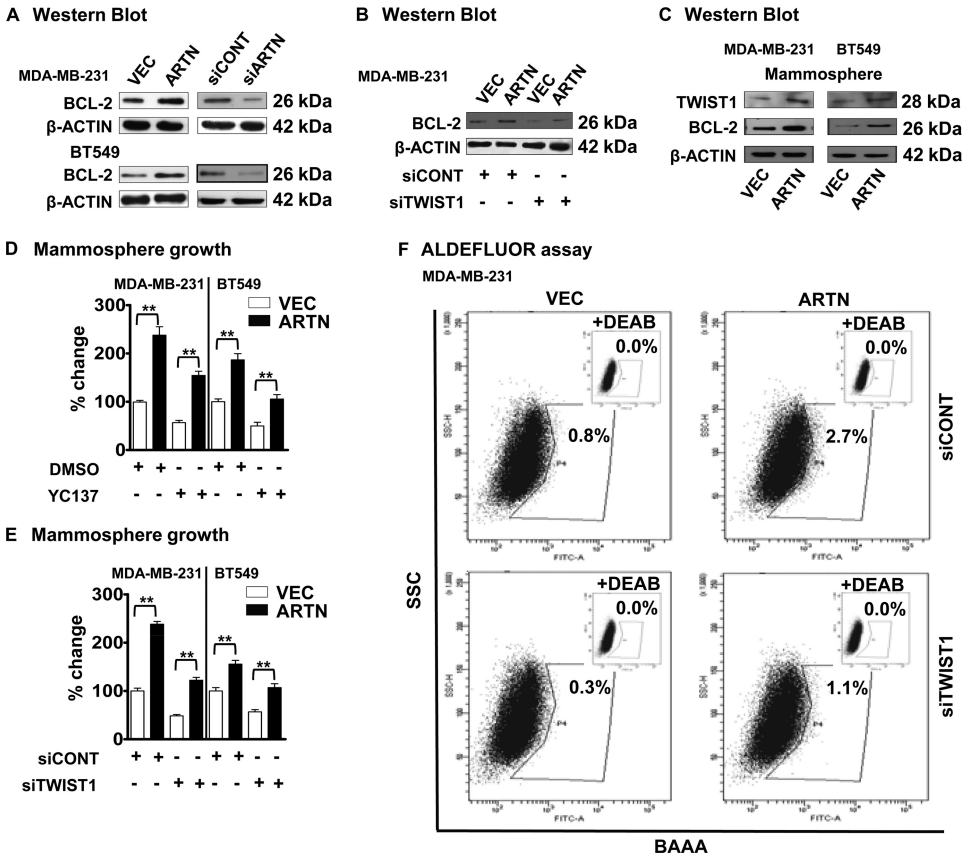

FIGURE 6. **ARTN increases BCL-2 expression to promote a CSC like phenotype in ER-MC cells.** *A*, Western blot determination of BCL-2 protein levels in MDA-MB-231 and BT549 cells with forced expression and depletion of ARTN is shown. β-Actin was used as a loading control for cell lysates. The sizes of the detected protein bands in kDa are shown on the *right*. *B*, Western blot determination of BCL-2 protein levels in MDA-MB-231 cells with forced expression of ARTN ± siRNA to TWIST1 is shown. β-Actin was used as loading control for cell lysates. The sizes of the detected protein bands in kDa are shown on the *right*. *C*, Western blot determination of TWIST1 and BCL-2 protein levels in MDA-MB-231 and BT549 cells with forced expression of ARTN grown under mammospheric conditions is shown. β-Actin was used as loading control for cell lysates. The sizes of the detected protein bands in kDa are shown on the *right*. *D*, mammospheric growth of MDA-MB-231 and BT549 cells with forced expression of ARTN was determined ± YC137 (5 μM). DMSO-treated VEC cells are presented as 100%. *E*, mammospheric growth of MDA-MB-231 and BT549 cells with forced expression of ARTN was determined ± siRNA to TWIST1. siCONT-treated VEC cells are presented as 100%. *F*, the Aldefluor assay was performed in MDA-MB-231 cells with forced expression of ARTN ± siRNA to TWIST1. Flow cytometry plots indicate side scatter (*SSC*) *versus* fluorescence intensity. **, $p < 0.01$.

ARTN cells (Fig. 6*D*). Next, to determine whether TWIST1 mediates ARTN stimulation of the CSC-like population, we employed siRNA to TWIST1 to selectively deplete TWIST1 expression in MDA-MB-231 and BT549 cells with forced expression of ARTN and their respective control VEC cells. Depletion of TWIST1 abrogated the stimulatory effects of ARTN on mammosphere formation in both MDA-MB-231-ARTN and BT549-ARTN cells (Fig. 6*E*). To determine whether ARTN utilized TWIST1 to increase the ALDH1+ population in ER-MC cells, we compared the percentage of ALDH1+ cells in MDA-MB-231-ARTN and MDA-MB-231-VEC cells ± siRNA to TWIST1. Depletion of TWIST1 reduced the basal percentages of the ALDH1+ population in MDA-MB-231-VEC cells. TWIST1 siRNA also largely abrogated the stimulatory effects of ARTN on the ALDH1+ cell population in MDA-MB-231-ARTN cells (Fig. 6*F*).

Next, we examined whether forced expression of TWIST1 would negate ARTN stimulation of increases in the CSC-like population. We performed the Aldefluor assay in BT549 cells stably transfected with TWIST1 and VEC-transfected control cells (14) ± siARTN. Depletion of ARTN by siRNA in BT549-VEC cells significantly decreased the percentage of the ALDH1+ cell population (supplemental Fig. S3). However, depletion of ARTN by siRNA in BT549-TWIST1 did not significantly alter the percentage of the ALDH1+ cell population. Thus, increased expression of TWIST1 and consequent stimulation of CSC-like behavior are downstream of ARTN stimulation.

ARTN-dependent Radio Resistance Is Mediated by BCL-2—Resistance to IR and chemotherapeutic agents is one characteristic of cells with CSC-like behavior (38). To determine if acquired resistance to IR in MDA-MB-231 cells resulted in an increased CSC-like population, we examined the mammospheric growth of MDA-MB-231-IRR cells compared with the WT cells. Concordant with published literature, MDA-MB-231-IRR cells exhibited an increased mammospheric cell growth (5, 8) and increased ALDH1+ cell populations (39) compared with the WT cells. siRNA-mediated depletion of ARTN resulted in decreased mammospheric cell growth and decreased ALDH1+ cell populations in both WT and IRR cells as compared with the respective siCONT cells (Fig. 7, *A* and *B*).

BCL-2 possesses a functional role in both radio- and chemoresistance (40, 41). Increased BCL-2 expression was observed in MDA-MB-231-IRR cells compared with the WT cells (Fig. 7*C*),

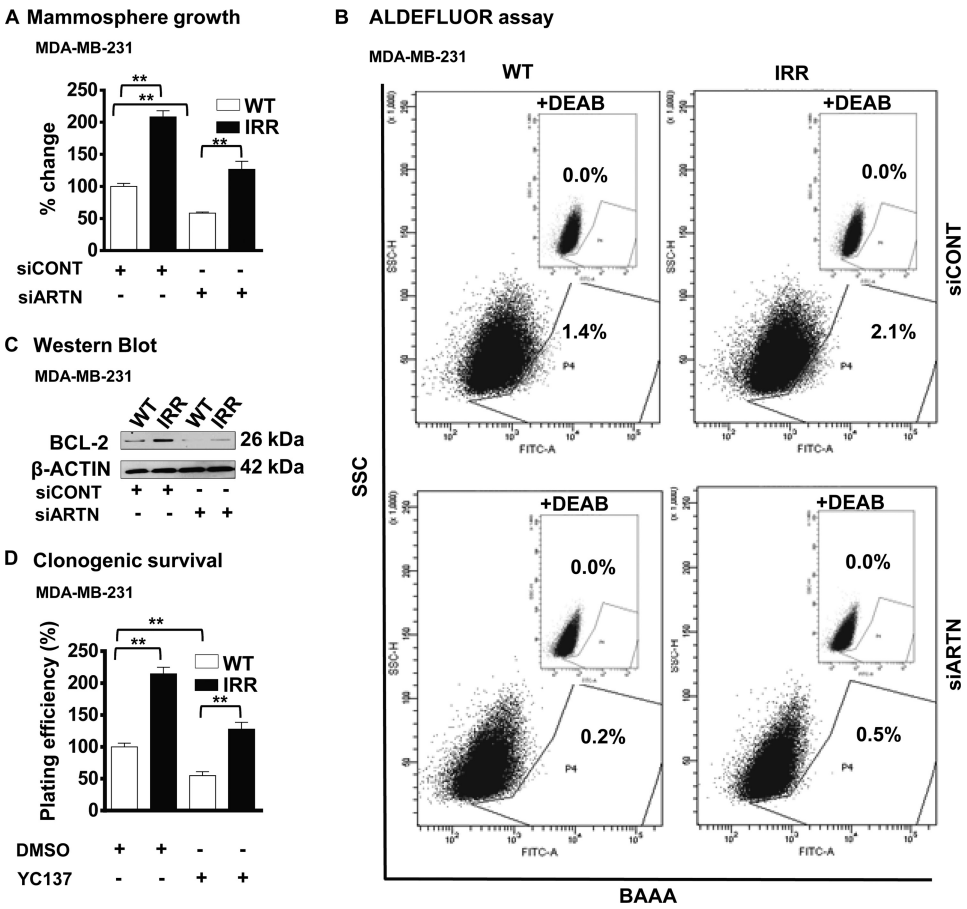

FIGURE 7. **BCL-2 is downstream of ARTN mediated acquired resistance to ionizing radiation and the increased CSC-like population in ER-MC cells.** *A*, MDA-MB-231-WT and -IRR cells were seeded in ultra low attachment plates in mammospheric growth media ± siRNA to ARTN. After 10 days, growth was measured by alamarBlue. Mammosphere formation by MDA-MB-231 IRR cells was increased as compared with respective WT cells. Depletion of ARTN by siARTN significantly decreased mammosphere formation in both IRR and WT cells of MDA-MB-231. *B*, ARTN-mediated acquired resistance to ionizing radiation resulted in an increased CSC-like population in ER-MC cells. Cells were incubated with Aldefluor substrate (BAAA, BODIPY®-aminoacetaldehyde) to define the Aldefluor-positive, and a specific inhibitor of ALDH1, diethylaminobenzaldehyde (*DEAB*), was used to establish the base-line fluorescence. Flow cytometry plots indicate side scatter (*SSC*) *versus* fluorescence intensity. The ALDH1+ cell population in MDA-MB-231 IRR cells was increased as compared with WT cells. Depletion of ARTN by siARTN significantly decreased the ALDH1+ cell population in IRR and WT cells of MDA-MB-231. *C*, Western blot was used to determine BCL-2 protein levels in MDA-MB-231-WT and -IRR ±siRNA to ARTN. β-Actin was used as the loading control for cell lysates. The sizes of the detected protein bands in kDa are shown on the *right*. *D*, clonogenic survival is shown. MDA-MB-231-WT and -IRR cells± YC137 were exposed to a 4-Gy dose of IR, and 24 h later, 600 cells/well were seeded in 10% serum-containing media in 6 well plates. After 2 weeks, colonies with greater than 50 cells were counted by crystal violet stain, and plating efficiencies were (number of colonies formed/number of cells seeded × 100. **, $p < 0.01$.

and siRNA-mediated depletion of ARTN resulted in decreased BCL-2 expression in both cell lines as compared with respective WT cells (Fig. 7*C*). To further determine whether ARTN dependent radio resistance is mediated by BCL-2, we treated MDA-MB-231-IRR and WT cells ± YC137 and performed a clonogenic assay. MDA-MB-231-IRR cells readily formed a higher number of colonies compared with the WT cells, and treatment with YC137 largely abrogated the increased number of colonies observed in the IR resistant cells (Fig. 7*D*).

ARTN and ALDH1 Are Co-expressed in ER-MC—ALDH1 expression in mammary carcinoma correlates with a poor survival outcome (31, 42). To determine a potential association between ARTN and ALDH1 expression in ER-MC, we first performed qPCR on a cohort of 24 ER-MC to compare the relative expression of ARTN mRNA and ALDH1 mRNA. We observed that ARTN mRNA expression was positively and highly correlated with ALDH1 mRNA expression (Pearson coefficient, 0.66; $p = 0.0008$) (Fig. 8*A*). We next determined a potential association of ARTN and ALDH1 protein expression in a cohort of 94 human ER-MC by immunohistochemistry and examined the association of expression. IHC analysis showed that both ARTN and ALDH1 protein were highly expressed in ER-MC. All 94 samples were positive for ALDH1 expression. We, therefore, stratified the samples according to the level of expression into two categories (low ALDH1 and high ALDH1 expression). As previously reported (31), patients whose tumors expressed high ALDH1 exhibited a worse survival outcome than those with low ALDH1 expression (supplemental Fig. S4). ARTN immunoreactivity was stratified according to the level of expression into four categories (negative, weak, moderate, and strong expression) (14). Of those tumors negative for ARTN expression, only 5.7% exhibited high ALDH1 expression. With increasing tumor expression of ARTN, there was a concordant graded increase in ALDH1 expression with 60% of tumors with strong ARTN expression also exhibiting high ALDH1 expression. To confirm the correlation of expression between ARTN and ALDH1 proteins in clinical samples, we compared the relationship by Spearman's rank correlation

A Correlation of ARTN and ALDH1 mRNA expression in ER- mammary carcinoma

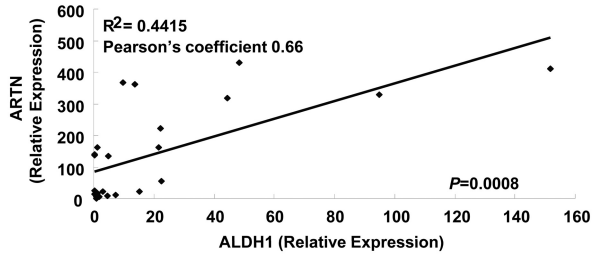

B Correlation of ARTN and ALDH1 protein expression in ER- mammary carcinoma

ARTN expression	ALDH1 expression: Low	ALDH1 expression: High
Negative	33 (94.3%)	2 (5.7%)
Weak	19 (65.5%)	10 (34.5%)
Moderate	10 (66.7%)	5 (33.3%)
Strong	6 (40%)	9 (60%)

Spearman correlation: $P = 0.001$ $r_s = 0.408$

C Correlation of ARTN and BCL-2 mRNA expression in ER- mammary carcinoma

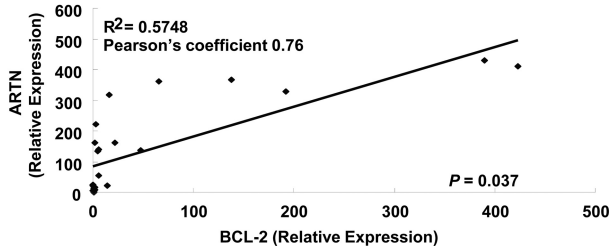

FIGURE 8. **Association of ARTN expression with ALDH1 or BCL-2 expression in ER-MC.** *A*, the Pearson correlation coefficient was determined between the mRNA expression of ARTN, and ALDH1 was determined by qPCR in a cohort of 24 patients with ER-MC. ARTN expression was positively correlated with ALDH1 expression ($\rho = 0.66$). *B*, shown is a correlation between ARTN and ALDH1 protein determined by IHC in a cohort of 94 patients with ER-MC. The expression parameters for ARTN have been described previously (14). *C*, Pearson correlation coefficient was determined between the mRNA expression of ARTN and BCL-2 determined by qPCR in a cohort of 24 ER-MC. ARTN expression was positively correlated with BCL-2 expression ($\rho = 0.76$).

coefficient and observed a significantly positive value (Spearman correlation, $r_s = 0.408$, $p = 0.001$) (Fig. 8*B*). Hence, ALDH1 expression in ER-MC is partially correlated with ARTN expression.

As ARTN regulated BCL-2 expression to stimulate CSC-like behavior in ER-MC cells, we also determined a potential association between ARTN and BCL-2 expression in ER-MC. By qPCR analysis on the same cohort of 24 ER-MC to compare the relative expression of ARTN mRNA and BCL-2 mRNA, we observed that ARTN mRNA expression was positively and highly correlated with BCL-2 mRNA expression (Pearson coefficient, 0.76; $p = 0.03$) (Fig. 8*C*). Hence, BCL-2 expression in ER-MC is also partially correlated with ARTN expression.

DISCUSSION

We have demonstrated herein that increased ARTN expression is associated with and functionally promotes acquired resistance of ER-MC cells to IR or paclitaxel concordant with the previously demonstrated role of ARTN in acquired resistance of ER+MC cells to tamoxifen (4). We also have preliminary evidence of a similar role for ARTN in HER2+ mammary carcinoma cell lines with acquired resistance to Herceptin.[5] The functional role of increased ARTN expression in resistant cells is apparently related to its capacity to enhance a CSC-like cell phenotype in ER-MC cell populations. CSC-like cells exhibit characteristics of EMT and are associated with greater metastatic potential (43). Similarly we have also previously demonstrated that ARTN stimulates an AKT-TWIST1-dependent EMT in ER-MC cells with a resultant increase in the metastatic potential of these cells (14). Increased expression of ARTN may, therefore, be a common adaptive mechanism used by cancer cells to promote cell survival and renewal in, and dispersal from, hostile microenvironments of different derivation.

To our knowledge, the work herein is the first demonstration of a member of the GDNF family of ligands (GFL), functioning as a CSC factor. However, other members of the GFL family have been demonstrated to regulate renewal of normal stem cell populations (44, 45). GDNF, for example, maintains spermatogonial stem cell renewal by paracrine secretion from Sertoli cells (44). GDNF signals through a multi-subunit receptor system composed of GFRα-1 or GFRα-3 and RET subunits that function as ligand binding and signaling components, respectively (46). ARTN has been reported to primarily utilize GFRα-3 (47) but has also been shown to bind to GFRα-1 (48) and also activates RET (48). Interestingly, GDNF has also been shown to signal via a RET-independent mechanism (49), and the cellular effects of GFLs may, therefore, be propagated through multiple independent pathways. A recent report demonstrated that GDNF and ARTN also interact with SYNDECAN-3, a transmembrane heparin sulfate proteoglycan with subsequent activation of Src kinase (50). SYNDECAN-3 is expressed in myogenic stem cells and cooperates with Notch to promote cell cycle progression and self-renewal and inhibit terminal differentiation (51). This alternate receptor for ARTN may be highly relevant in the context that the MDA-MB-231 cell line used herein does not express RET (52), and therefore, the observed effects of ARTN on the CSC-like phenotype in these cells are RET independent. The expression of the three identified ARTN receptors (GFRα-1, GFRα-3, and SYNDECAN-3) in mammary carcinoma and their potential significance in prognosis of mammary carcinoma is currently under investigation.[6] Regardless of which receptor pathways initiate ARTN signaling in ER-MC cells, it is apparent that ARTN stimulation of both the EMT (14) and CSC-like phenotypes is mediated by TWIST1. TWIST1 has been demonstrated to be essential to promote EMT and tumor initiating capacity (53). *BMI1* is a downstream transcriptional target for TWIST1 in head and neck squamous cell carcinoma (53). We have observed that ARTN also stimulates *BMI1* expression via TWIST1 in ER-MC cells (data not shown). Furthermore, TWIST1 has been demonstrated to be sufficient to promote invadopodia formation leading to metastasis of mammary carcinoma cells (54). The centrality of TWIST1 for the cellular response to ARTN is also evidenced by

[5] K. S. Ding, Y. Yuan, Y. L. Yang, R. Li, V. Pandey, P. E. Lobie, and T. Zhu, manuscript in preparation.

[6] Z. S. Wu, V. Pandey, W. Y. Wu, S. Ye, T. Zhu, and P. E. Lobie, manuscript in preparation.

the previous observation that combined low expression of both ARTN and TWIST1 in ER-MC predicts 100% patient survival in contrast to poor survival outcome of patients with tumors that express both high ARTN and high TWIST1 (14).

Involvement of BCL-2 in mammary carcinoma correlates with both favorable prognosis in early stage mammary carcinoma (55) and poorer prognosis associated with increased invasive potential in triple negative (TN) mammary carcinoma, where it has been demonstrated that in TN mammary carcinoma BCL-2 is associated with poorer survival outcome (56). Furthermore, BCL-2 is also associated with increased therapeutic resistance (57) and promotion of breast cancer-initiating cells (17). Significantly, in patients with ER+ tumors treated with tamoxifen, increased BCL-2 expression was highly associated with a significantly worse survival outcome (58). Similarly, increased expression of ARTN has been reported to be associated with a worse survival outcome in such patients, an effect mediated by BCL-2 (4).

Regardless of its prognostic value, BCL-2, although necessary, is clearly not the sole functional promoter of the CSC-like actions of ARTN. Indeed, expression analyses indicate that ARTN modulates the expression of a range of genes potentially involved in promoting CSC-like behavior (14). Furthermore, BCL-2 has multiple interacting partners such as BAK, BAX, and BAD, and the relative expression ratios of BCL-2 to these inhibitory partners exert significant effects on BCL-2 function (59) and undoubtedly the prognostic significance of BCL-2 expression. It is, therefore, interesting that ARTN has previously been demonstrated to regulate BAX in both mammary (13) and endometrial carcinoma cells (15). Hence, although BCL-2 expression by itself may be associated with a good prognosis, the expression of other interacting proteins and pathways will determine the final functional effect of BCL-2 expression in tumors. As indicated above and in numerous other studies (60), inhibition of BCL-2 increases tumor cell sensitivity to apoptosis.

Furthermore, consistent with published literature (17, 40, 41), we have also shown here that BCL-2 mediates ARTN acquired radio-and chemo-resistance and the CSC-like characteristics in ER-MC cells. ARTN expression was significantly and positively correlated with BCL-2 expression in a cohort of ER-MC. The involvement of TWIST1 in radio-and chemo-resistance and CSC-like characteristics in mammary carcinoma is also evident from the literature (16) as is AKT regulation of both TWIST1 and BCL-2 (14, 61). Depletion of TWIST1 leads to increased sensitivity to taxol in prostate cancer cells and was associated with down-regulation of BCL-2 and subsequent activation of apoptosis (37). Concordantly, we demonstrated ARTN utilizes TWIST1 to transcriptionally regulate BCL-2. Thus, BCL-2 is a downstream target of ARTN via TWIST1. Previous reports also suggested that TWIST1 increases VEGF gene expression in patients with metastatic mammary carcinoma (62). VEGF has been reported to increase BCL-2 expression in human and murine mammary adenocarcinoma cells (63). Collectively, we can conclude that ARTN activates AKT with consequent increased expression of TWIST1 and BCL-2 to promote radio-and chemo-resistance via increasing CSC-like behavior of ER-MC cells.

In summary we have demonstrated a functional role of ARTN in acquired resistance to paclitaxel and IR by promotion of a CSC-like cell phenotype in mammary carcinoma cells. ARTN expression in mammary carcinoma could, therefore, be interrogated as a marker along with TWIST1 (14) to identify those patients likely to experience resistance to therapy and recurrence. Furthermore, combined inhibition of ARTN and PI3K/AKT/TWIST1/BCL-2 could be considered as one potential approach to limit development of acquired resistance to multiple therapeutic strategies used to treat mammary carcinoma.

REFERENCES

1. Chen, J.-Q., and Russo, J. (2009) ERα-negative and triple negative breast cancer. Molecular features and potential therapeutic approaches. *Biochim. Biophys. Acta* **1796,** 162–175
2. Dent, R., Trudeau, M., Pritchard, K. I., Hanna, W. M., Kahn, H. K., Sawka, C. A., Lickley, L. A., Rawlinson, E., Sun, P., and Narod, S. A. (2007) Triple-negative breast cancer. Clinical features and patterns of recurrence. *Clin. Cancer Res.* **13,** 4429–4434
3. Arpino, G., Wiechmann, L., Osborne, C. K., and Schiff, R. (2008) Crosstalk between the estrogen receptor and the HER tyrosine kinase receptor family. Molecular mechanism and clinical implications for endocrine therapy resistance. *Endocr. Rev.* **29,** 217–233
4. Kang, J., Qian, P. X., Pandey, V., Perry, J. K., Miller, L. D., Liu, E. T., Zhu, T., Liu, D. X., and Lobie, P. E. (2010) Artemin is estrogen-regulated and mediates anti-estrogen resistance in mammary carcinoma. *Oncogene* **29,** 3228–3240
5. Dean, M., Fojo, T., and Bates, S. (2005) Tumour stem cells and drug resistance. *Nat. Rev. Cancer* **5,** 275–284
6. Mani, S. A., Guo, W., Liao, M. J., Eaton, E. N., Ayyanan, A., Zhou, A. Y., Brooks, M., Reinhard, F., Zhang, C. C., Shipitsin, M., Campbell, L. L., Polyak, K., Brisken, C., Yang, J., and Weinberg, R. A. (2008) The epithelial-mesenchymal transition generates cells with properties of stem cells. *Cell* **133,** 704–715
7. Scheel, C., Eaton, E. N., Li, S. H., Chaffer, C. L., Reinhardt, F., Kah, K. J., Bell, G., Guo, W., Rubin, J., Richardson, A. L., and Weinberg, R. A. (2011) Paracrine and autocrine signals induce and maintain mesenchymal and stem cell states in the breast. *Cell* **145,** 926–940
8. Baumann, M., Krause, M., and Hill, R. (2008) Exploring the role of cancer stem cells in radioresistance. *Nat. Rev. Cancer* **8,** 545–554
9. Rakha, E. A., Reis-Filho, J. S., and Ellis, I. O. (2008) Basal-like breast cancer. A critical review. *J. Clin. Oncol.* **26,** 2568–2581
10. Prat, A., Parker, J. S., Karginova, O., Fan, C., Livasy, C., Herschkowitz, J. I., He, X., and Perou, C. M. (2010) Phenotypic and molecular characterization of the claudin-low intrinsic subtype of breast cancer. *Breast Cancer Res.* **12,** R68
11. Taube, J. H., Herschkowitz, J. I., Komurov, K., Zhou, A. Y., Gupta, S., Yang, J., Hartwell, K., Onder, T. T., Gupta, P. B., Evans, K. W., Hollier, B. G., Ram, P. T., Lander, E. S., Rosen, J. M., Weinberg, R. A., and Mani, S. A. (2010) Core epithelial-to-mesenchymal transition interactome gene-expression signature is associated with claudin-low and metaplastic breast cancer subtypes. *Proc. Natl. Acad. Sci. U.S.A.* **107,** 15449–15454
12. Gao, M. Q., Choi, Y. P., Kang, S., Youn, J. H., and Cho, N. H. (2010) CD24+ cells from hierarchically organized ovarian cancer are enriched in cancer stem cells. *Oncogene* **29,** 2672–2680
13. Kang, J., Perry, J. K., Pandey, V., Fielder, G. C., Mei, B., Qian, P. X., Wu, Z. S., Zhu, T., Liu, D. X., and Lobie, P. E. (2009) Artemin is oncogenic for human mammary carcinoma cells. *Oncogene* **28,** 2034–2045
14. Banerjee, A., Wu, Z. S., Qian, P., Kang, J., Pandey, V., Liu, D. X., Zhu, T., and Lobie, P. E. (2011) Artemin synergizes with TWIST1 to promote metastasis and poor survival outcome in patients with ER negative mammary carcinoma. *Breast Cancer Res.* **13,** R112
15. Pandey, V., Jung, Y., Kang, J., Steiner, M., Qian, P. X., Banerjee, A., Mitchell, M. D., Wu, Z. S., Zhu, T., Liu, D. X., and Lobie, P. E. (2010) Artemin reduces sensitivity to doxorubicin and paclitaxel in endometrial carcinoma cells through specific regulation of CD24. *Transl. Oncol.* **3,** 218–229

16. Vesuna, F., Lisok, A., Kimble, B., and Raman, V. (2009) Twist modulates breast cancer stem cells by transcriptional regulation of CD24 expression. *Neoplasia* **11,** 1318–1328
17. Lang, J. Y., Hsu, J. L., Meric-Bernstam, F., Chang, C. J., Wang, Q., Bao, Y., Yamaguchi, H., Xie, X., Woodward, W. A., Yu, D., Hortobagyi, G. N., and Hung, M. C. (2011) BikDD eliminates breast cancer initiating cells and synergizes with lapatinib for breast cancer treatment. *Cancer Cell* **20,** 341–356
18. Liu, G., Yuan, X., Zeng, Z., Tunici, P., Ng, H., Abdulkadir, I. R., Lu, L., Irvin, D., Black, K. L., and Yu, J. S. (2006) Analysis of gene expression and chemoresistance of CD133+ cancer stem cells in glioblastoma. *Mol. Cancer* **5,** 67
19. Tang, J.-Z., Kong, X.-J., Kang, J., Fielder, G. C., Steiner, M., Perry, J. K., Wu, Z.-S., Yin, Z., Zhu, T., Liu, D.-X., and Lobie, P. E. (2010) Artemin-stimulated progression of human non-small cell lung carcinoma is mediated by BCL2. *Mol. Cancer Ther.* **9,** 1697–1708
20. Lo, H. W., Hsu, S. C., Xia, W., Cao, X., Shih, J. Y., Wei, Y., Abbruzzese, J. L., Hortobagyi, G. N., and Hung, M. C. (2007) Epidermal growth factor receptor cooperates with signal transducer and activator of transcription 3 to induce epithelial-mesenchymal transition in cancer cells via up-regulation of TWIST gene expression. *Cancer Res.* **67,** 9066–9076
21. Liu, D. X., and Lobie, P. E. (2007) Transcriptional activation of p53 by Pitx1. *Cell Death Differ* **14,** 1893–1907
22. Olive, P. L., and Banáth, J. P. (2006) The comet assay. A method to measure DNA damage in individual cells. *Nat. Protoc.* **1,** 23–29
23. Franken, N. A., Rodermond, H. M., Stap, J., Haveman, J., and van Bree, C. (2006) Clonogenic assay of cells *in vitro*. *Nat. Protoc.* **1,** 2315–2319
24. Karimi-Busheri, F., Zadorozhny, V., Shawler, D. L., and Fakhrai, H. (2010) The stability of breast cancer progenitor cells during cryopreservation. Maintenance of proliferation, self-renewal, and senescence characteristics. *Cryobiology* **60,** 308–314
25. Deans, A. J., Khanna, K. K., McNees, C. J., Mercurio, C., Heierhorst, J., and McArthur, G. A. (2006) Cyclin-dependent kinase 2 functions in normal DNA repair and is a therapeutic target in BRCA1-deficient cancers. *Cancer Res.* **66,** 8219–8226
26. Pearce, A. G., Segura, T. M., Rintala, A. C., Rintala-Maki, N. D., and Lee, H. (2001) The generation and characterization of a radiation-resistant model system to study radioresistance in human breast cancer cells. *Radiat. Res.* **156,** 739–750
27. Patel, N., Chatterjee, S. K., Vrbanac, V., Chung, I., Mu, C. J., Olsen, R. R., Waghorne, C., and Zetter, B. R. (2010) Rescue of paclitaxel sensitivity by repression of Prohibitin1 in drug-resistant cancer cells. *Proc. Natl. Acad. Sci. U.S.A.* **107,** 2503–2508
28. Liu, S., Dontu, G., and Wicha, M. S. (2005) Mammary stem cells, self-renewal pathways, and carcinogenesis. *Breast Cancer Res.* **7,** 86–95
29. Song, J., Chang, I., Chen, Z., Kang, M., and Wang, C. Y. (2010) Characterization of side populations in HNSCC. Highly invasive, chemo-resistant, and abnormal Wnt signaling. *PLoS ONE* **5,** e11456
30. Takahashi-Yanaga, F., and Kahn, M. (2010) Targeting Wnt signaling. Can we safely eradicate cancer stem cells? *Clin. Cancer Res.* **16,** 3153–3162
31. Ginestier, C., Hur, M. H., Charafe-Jauffret, E., Monville, F., Dutcher, J., Brown, M., Jacquemier, J., Viens, P., Kleer, C. G., Liu, S., Schott, A., Hayes, D., Birnbaum, D., Wicha, M. S., and Dontu, G. (2007) ALDH1 is a marker of normal and malignant human mammary stem cells and a predictor of poor clinical outcome. *Cell Stem Cell* **1,** 555–567
32. Korkaya, H., Paulson, A., Charafe-Jauffret, E., Ginestier, C., Brown, M., Dutcher, J., Clouthier, S. G., and Wicha, M. S. (2009) Regulation of mammary stem/progenitor cells by PTEN/Akt/β-catenin signaling. *PLoS Biol* **7,** e1000121
33. Korkaya, H., Paulson, A., Iovino, F., and Wicha, M. S. (2008) HER2 regulates the mammary stem/progenitor cell population driving tumorigenesis and invasion. *Oncogene* **27,** 6120–6130
34. Croker, A. K., Goodale, D., Chu, J., Postenka, C., Hedley, B. D., Hess, D. A., and Allan, A. L. (2009) High aldehyde dehydrogenase and expression of cancer stem cell markers selects for breast cancer cells with enhanced malignant and metastatic ability. *J. Cell Mol. Med.* **13,** 2236–2252
35. Clarke, M. F., and Fuller, M. (2006) Stem cells and cancer. Two faces of eve. *Cell* **124,** 1111–1115
36. Ansieau, S., Morel, A. P., Hinkal, G., Bastid, J., and Puisieux, A. (2010) TWISTing an embryonic transcription factor into an oncoprotein. *Oncogene* **29,** 3173–3184
37. Kwok, W. K., Ling, M. T., Lee, T. W., Lau, T. C., Zhou, C., Zhang, X., Chua, C. W., Chan, K. W., Chan, F. L., Glackin, C., Wong, Y. C., and Wang, X. (2005) Up-regulation of TWIST in prostate cancer and its implication as a therapeutic target. *Cancer Res.* **65,** 5153–5162
38. Morrison, R., Schleicher, S. M., Sun, Y., Niermann, K. J., Kim, S., Spratt, D. E., Chung, C. H., and Lu, B. (2011) Targeting the mechanisms of resistance to chemotherapy and radiotherapy with the cancer stem cell hypothesis. *J. Oncol.* 2011, 941876
39. Foubert, E., De Craene, B., and Berx, G. (2010) Key signalling nodes in mammary gland development and cancer. The Snail1-Twist1 conspiracy in malignant breast cancer progression. *Breast Cancer Res.* **12,** 206
40. Gazitt, Y., Rothenberg, M. L., Hilsenbeck, S. G., Fey, V., Thomas, C., and Montegomrey, W. (1998) Bcl-2 overexpression is associated with resistance to paclitaxel, but not gemcitabine, in multiple myeloma cells. *Int. J. Oncol.* **13,** 839–848
41. Jameel, J. K., Rao, V. S., Cawkwell, L., and Drew, P. J. (2004) Radioresistance in carcinoma of the breast. *Breast* **13,** 452–460
42. Morimoto, K., Kim, S. J., Tanei, T., Shimazu, K., Tanji, Y., Taguchi, T., Tamaki, Y., Terada, N., and Noguchi, S. (2009) Stem cell marker aldehyde dehydrogenase 1-positive breast cancers are characterized by negative estrogen receptor, positive human epidermal growth factor receptor type 2, and high Ki67 expression. *Cancer Sci* **100,** 1062–1068
43. May, C. D., Sphyris, N., Evans, K. W., Werden, S. J., Guo, W., and Mani, S. A. (2011) Epithelial-mesenchymal transition and cancer stem cells. A dangerously dynamic duo in breast cancer progression. *Breast Cancer Res.* **13,** 202
44. Hofmann, M. C. (2008) Gdnf signaling pathways within the mammalian spermatogonial stem cell niche. *Mol. Cell. Endocrinol.* **288,** 95–103
45. Spinnler, K., Köhn, F. M., Schwarzer, U., and Mayerhofer, A. (2010) Glial cell line-derived neurotrophic factor is constitutively produced by human testicular peritubular cells and may contribute to the spermatogonial stem cell niche in man. *Hum. Reprod.* **25,** 2181–2187
46. Airaksinen, M. S., and Saarma, M. (2002) The GDNF family. Signaling, biological functions. and therapeutic value. *Nat. Rev. Neurosci.* **3,** 383–394
47. Bespalov, M. M., and Saarma, M. (2007) GDNF family receptor complexes are emerging drug targets. *Trends Pharmacol. Sci.* **28,** 68–74
48. Baloh, R. H., Gorodinsky, A., Golden, J. P., Tansey, M. G., Keck, C. L., Popescu, N. C., Johnson, E. M., Jr., and Milbrandt, J. (1998) GFRα3 is an orphan member of the GDNF/neurturin/persephin receptor family. *Proc. Natl. Acad. Sci. U.S.A.* **95,** 5801–5806
49. Rangasamy, S. B., Soderstrom, K., Bakay, R. A., and Kordower, J. H. (2010) Neurotrophic factor therapy for Parkinson's disease. *Prog. Brain Res.* **184,** 237–264
50. Bespalov, M. M., Sidorova, Y. A., Tumova, S., Ahonen-Bishopp, A., Magalhães, A. C., Kulesskiy, E., Paveliev, M., Rivera, C., Rauvala, H., and Saarma, M. (2011) Heparan sulfate proteoglycan syndecan-3 is a novel receptor for GDNF, neurturin, and artemin. *J. Cell Biol.* **192,** 153–169
51. Pisconti, A., Cornelison, D. D., Olguín, H. C., Antwine, T. L., and Olwin, B. B. (2010) Syndecan-3 and Notch cooperate in regulating adult myogenesis. *J. Cell Biol.* **190,** 427–441
52. Boulay, A., Breuleux, M., Stephan, C., Fux, C., Brisken, C., Fiche, M., Wartmann, M., Stumm, M., Lane, H. A., and Hynes, N. E. (2008) The Ret receptor tyrosine kinase pathway functionally interacts with the ERα pathway in breast cancer. *Cancer Res.* **68,** 3743–3751
53. Yang, M. H., Hsu, D. S., Wang, H. W., Wang, H. J., Lan, H. Y., Yang, W. H., Huang, C. H., Kao, S. Y., Tzeng, C. H., Tai, S. K., Chang, S. Y., Lee, O. K., and Wu, K. J. (2010) Bmi1 is essential in Twist1-induced epithelial-mesenchymal transition. *Nat. Cell Biol.* **12,** 982–992
54. Eckert, M. A., Lwin, T. M., Chang, A. T., Kim, J., Danis, E., Ohno-Machado, L., and Yang, J. (2011) Twist1-induced invadopodia formation promotes tumor metastasis. *Cancer Cell* **19,** 372–386
55. Dawson, S. J., Makretsov, N., Blows, F. M., Driver, K. E., Provenzano, E., Le Quesne, J., Baglietto, L., Severi, G., Giles, G. G., McLean, C. A., Callagy, G., Green, A. R., Ellis, I., Gelmon, K., Turashvili, G., Leung, S., Aparicio, S., Huntsman, D., Caldas, C., and Pharoah, P. (2010) BCL2 in breast cancer. A

favourable prognostic marker across molecular subtypes and independent of adjuvant therapy received. *Br. J. Cancer* **103,** 668–675
56. Tawfik, K., Kimler, B. F., Davis, M. K., Fan, F., and Tawfik, O. (2012) Prognostic significance of Bcl-2 in invasive mammary carcinomas. A comparative clinicopathologic study between "triple-negative" and non-"triple-negative" tumors. *Hum. Pathol.* **43,** 23–30
57. Yang, Q., Moran, M. S., and Haffty, B. G. (2009) Bcl-2 expression predicts local relapse for early-stage breast cancer receiving conserving surgery and radiotherapy. *Breast Cancer Res. Treat* **115,** 343–348
58. Kerr, D. A., 2nd, and Wittliff, J. L. (2011) A five-gene model predicts clinical outcome in ER+/PR+, early-stage breast cancers treated with adjuvant tamoxifen. *Horm. Cancer* **2,** 261–271
59. Youle, R. J., and Strasser, A. (2008) The BCL-2 protein family. Opposing activities that mediate cell death. *Nat. Rev. Mol. Cell Biol.* **9,** 47–59
60. Samuel, S., Tumilasci, V. F., Oliere, S., Nguyên, T. L., Shamy, A., Bell, J., and Hiscott, J. (2010) VSV oncolysis in combination with the BCL-2 inhibitor obatoclax overcomes apoptosis resistance in chronic lymphocytic leukemia. *Mol. Ther.* **18,** 2094–2103
61. Bratton, M. R., Duong, B. N., Elliott, S., Weldon, C. B., Beckman, B. S., McLachlan, J. A., and Burow, M. E. (2010) Regulation of ERα-mediated transcription of Bcl-2 by PI3K-AKT cross-talk: implications for breast cancer cell survival. *Int. J. Oncol.* **37,** 541–550
62. Kallergi, G., Papadaki, M. A., Politaki, E., Mavroudis, D., Georgoulias, V., and Agelaki, S. (2011) Epithelial to mesenchymal transition markers expressed in circulating tumorcells of early and metastatic breast cancer patients. *Breast Cancer Res.* **13,** R59
63. Pidgeon, G. P., Barr, M. P., Harmey, J. H., Foley, D. A., and Bouchier-Hayes, D. J. (2001) Vascular endothelial growth factor (VEGF) up-regulates BCL-2 and inhibits apoptosis in human and murine mammary adenocarcinoma cells. *Br. J. Cancer* **85,** 273–278